Supporting Information

High-efficiency Catalyst $CuSO_4$/SBA-15 Toward Butylated Hydroxytoluene Synthesis in Heterogeneous System

Yi-Jie Wang,[a] Yu-Fen Bao,[a] Xiao-Jie Lu,[a] Jia-Qi Dong[a] and Ding-Hua Liu*[a]

[a] State Key Laboratory of Materials-Oriented Chemical Engineering, College of Chemical Engineering, Nanjing Tech University, Nanjing 210009, China

*Corresponding authors: Ding-Hua Liu

E-mail: ncldh@njtech.edu.cn

1. Catalyst characterization

Low- and wide-angle powder X-ray diffraction (XRD) patterns of the catalysts were recorded on a Bruker D8-Advance diffractometer using Cu Kα (λ = 0.154 nm) radiation. Analysis was performed in the 2θ range from 0.1° to 4° (low angle) and from 10° to 80° (wide angle) with a scan rate of 0.02 °/s. The chemical states of catalysts were detected by X-ray photoelectron spectroscopy (XPS, PHI 550). The measured spectra were corrected for peak position with C1s (284.6 eV) using Al as the target ray source. The samples were degassed at 373 K for 6 h and the adsorption-desorption isotherms were recorded at 77 K using a MicrotracBEL BELSORP-MAX II specific surface area and pore size analyzer. The specific surface area was calculated using the BET method, and the pore volumes were calculated from the corresponding desorption isotherms. The pore size distributions were estimated using the Barrett, Joyner, and Halenda (BJH) algorithm. The Fourier infrared spectra (FT-IR) of the catalysts were measured with a Thermo Fisher NICOLEIS10 infrared spectrometer, using anhydrous KBr as a standard. The mass ratio of catalyst to KBr was 100:1, the scanning wavenumber range was 500-4000 cm^{-1}, and the number of scans was 64. Thermogravimetric analysis (TG) of the catalysts was performed on a NETZSCH STA-499F3 thermal analyzer. From room temperature to 900 °C at 10 °C/min, air with a flow rate of 20 mL/min was taken as a carrier gas and N_2 as a protective gas. The ultrastructure of the catalysts was analyzed using a Tecnai G2 F20 transmission electron microscope (TEM) with an operating voltage of 200 KV.

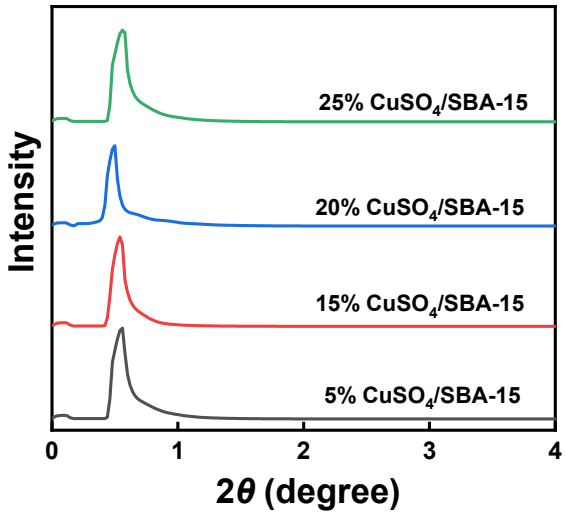

Figure S1. Small-angle XRD patterns of $CuSO_4$/SBA-15

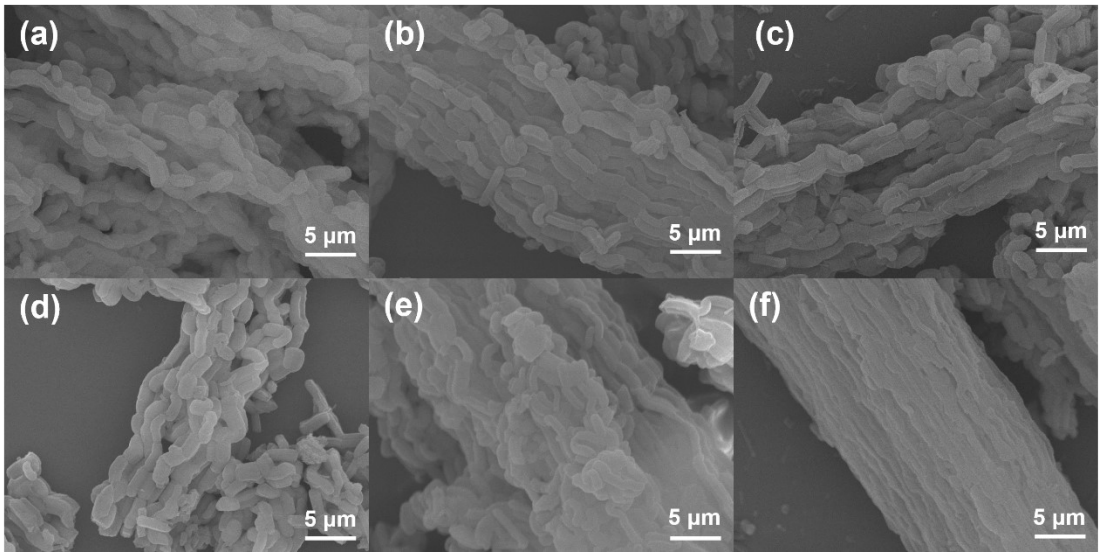

Figure S2. SEM images of (a) SBA-15, (b) 5%$CuSO_4$/SBA-15, (c) 10%$CuSO_4$/SBA-15, (d) 15%$CuSO_4$/SBA-15, (e) 20%$CuSO_4$/SBA-15 and (f) 25%$CuSO_4$/SBA-15

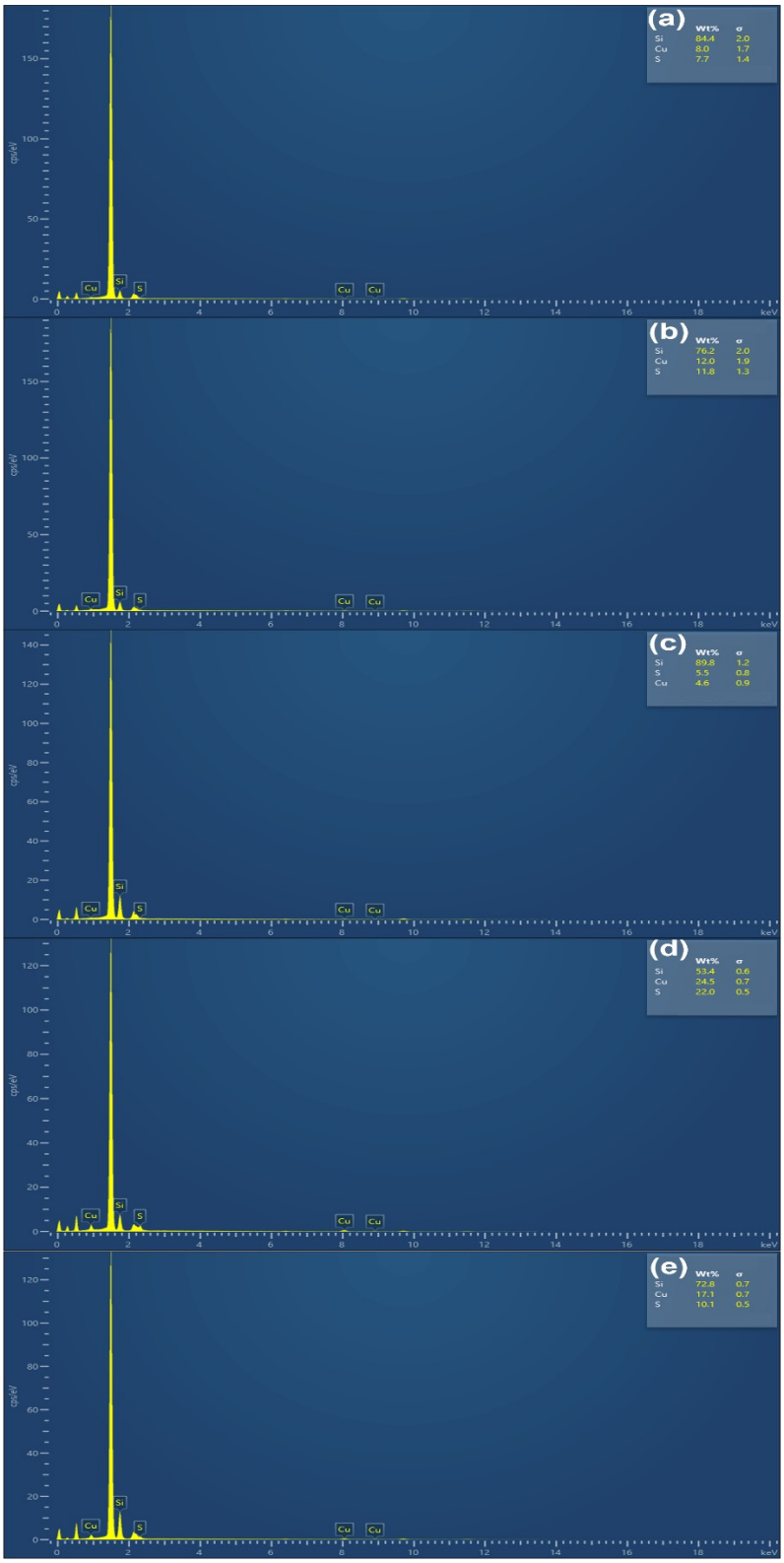

Figure S3. EDS elemental analysis of $CuSO_4$//SBA-15 catalysts: (a) 5% $CuSO_4$/SBA-15, (b) 10% $CuSO_4$/SBA-15, (c) 15% $CuSO_4$/SBA-15, (d) 20% $CuSO_4$/SBA-15 and (e) 25% $CuSO_4$/SBA-15.

Table S1. Effect of reaction time on the yield of BHT.

Reaction time (h)	Yield (%)
0.5	12.8
1.5	70.2
2.5	80.2
3.5	84.4
4.5	85.4

Table S2. Effect of reaction temperature on the yield of BHT.

Reaction temperature (°C)	Yield (%)
40	45.9
60	69.4
80	81.7
100	76.7
120	70.1

Table S3. Activity of various supported $CuSO_4$/SBA-15 catalysts.

Catalyst	Yield (%)
$CuSO_4$	0
5%$CuSO_4$/SBA-15	72.9
10%$CuSO_4$/SBA-15	85.5
15%$CuSO_4$/SBA-15	77.8
20%$CuSO_4$/SBA-15	71.3
25%$CuSO_4$/SBA-15	70.1

Table S4. Cycling stability of the catalyst.

Reaction cycle	Yield (%)
1	85.5
2	81.7
3	81.3
4	72.9
5	83.7

Table S5. Catalytic activity of various catalysts.

Catalyst	Yield (%)
/	0
$CuSO_4$	3.2
$CuSO_4$/SBA-15	85.5
sulfated SBA-15	71.6

Table S6. Catalytic activity of different mesoporous silica carriers.

Catalyst	Yield (%)
$CuSO_4$/SBA-15	85.5
$CuSO_4$/mesoporous SiO_2-1	84.6
$CuSO_4$/mesoporous SiO_2-2	73.5

Table S7. Physicochemical properties of different carriers.

Sample Name	BET Surface Area(m^2/g)	Pore Volume (cm^3/g)	Average Pore Size (nm)
SBA-15	832	1.09	5.22
mesoporous SiO_2-1	236	0.28	2.3
mesoporous SiO_2-2	61	0.12	2.1

Table S8. Cycling stability of $CuSO_4$/mesoporous SiO_2-1.

Reaction cycle	Yield (%)
1	83.8
2	57.1
3	19.2
4	12.9

Table S9. Cycling stability of $CuSO_4$/mesoporous SiO_2-2.

Reaction cycle	Yield (%)
1	73.5
2	62.2
3	23.3
4	10.9

Table S10. Activity of various Lewis acid loaded catalysts.

Catalyst	Yield (%)
$Fe_2(SO_4)_3$/SBA-15	83.8
$CuSO_4$/SBA-15	85.5
$Ce(SO_4)_2$/SBA-15	82.6

Table S11. Cycling stability of $Fe_2(SO_4)_3$/SBA-15.

Reaction cycle	Yield (%)
1	83.8
2	84.2
3	76.2
4	40.2

Table S12. Cycling stability of $Ce(SO_4)_2$/SBA-15.

Reaction cycle	Yield (%)
1	82.6
2	78.2
3	73.4
4	35.5